NAIST-IS-MT1651062

Master's Thesis

Maximum Achievable Efficiency for Multiple-Receiver Inductive Power Transfer Systems

Reona Sugiyama

February 1, 2018

Graduate School of Information Science
Nara Institute of Science and Technology

A Master's Thesis
submitted to Graduate School of Information Science,
Nara Institute of Science and Technology
in partial fulfillment of the requirements for the degree of
MASTER of ENGINEERING

Reona Sugiyama

Thesis Committee:

Professor Minoru Okada	(Supervisor)
Professor Kenji Sugimoto	(Co-supervisor)
Associate Professor Takeshi Higashino	(Co-supervisor)
Assistant Professor Thang Duong Quang	(Co-supervisor)

Maximum Achievable Efficiency for Multiple-Receiver Inductive Power Transfer Systems∗

Reona Sugiyama

Abstract

This work is to establish principles for design and benchmarking multiple-receiver inductive power transfer (IPT) system. We derive the formulas for obtaining optimal loads impedance of multiple-receivers and maximum power transmission efficiency based on N-port network model. Via theoretical analysis, electromagnetic simulation and experiment, we clarify that the cross-coupling among receivers does not deteriorate system efficiency if load resistance and reactance are jointly optimized. We also prove that the maximum efficiency which is newly introduced as system kQ-product in this work, equals to the sum of squares of kQ-product of individual transmitter-receiver link. The efficiency can be expressed by an efficiency angle tangent, in a manner analogous to the well-known kQ-product of single-receiver IPT. In the experimental verification, we measured an extensive S-parameter to validate the derived formulas. This experiment investigated two and three receiver IPT system because of the limitation of equipment, however, these results contribute to establish the kQ-theory for more than four multi-receiver IPT systems.

Keywords:

inductive power transfer, multiple-receiver, optimal loads, maximum achievable efficiency, kQ-product

∗Master's Thesis, Graduate School of Information Science,
Nara Institute of Science and Technology, NAIST-IS-MT1651062, March 13, 2018.

Contents

List of Figures

List of Tables

1 Introduction

1.1 Background and motivations

In 2007, the Witricity team at the Massachusetts Institute of Technology (MIT) succeeded in wirelessly supplying power to a 60 W bulb at a distance of 2 meters [1]. The main techniques of the experiment are "electromagnetic induction of Faraday" and "resonance", and the technology combining these is called IPT. Until 2007, it was applicable only to applications using short-range wireless power transmission such as RFID [2]. But since 2007, highly efficient and long distance wireless power transmission is enabled by the IPT system [3]. It is used for automobiles (EV), automatic (AGV), smart phones, wireless sensor networks, etc..., and the range of applications is expanding [4]. Therefore, the IPT system is currently drawing attention from many researchers and companies [5]. However, there is a concern about the loss of power transmission accompanying cordlessness, each companies are actively engaged in high efficiency [6]. Therefore, maximum efficiency is an important parameter as an indicator at product development stage. In addition, it is important according to that the parameter is the kQ-product [7]. As a recent example, D-Broad EV [8] is the first product of DAIHEN with a maximum AC input of 11 kW corresponding to Society of Automotive Engineers (SAE) [9]. The maximum transmission efficiency of this product is 92%. It is also possible to shift from 100 mm to 250 mm between the transmitting coil and the receiving coil.

Efficiency maximization for inductive power transfer (IPT) systems [10] is a complicated design optimization of transmit-receive coil system, conversion circuits and loading. Fortunately, the concept of maximum achievable efficiency and optimal load [7]– [11] facilitates this process by decoupling the design for the coils from those for the others. It has been shown that the optimal load reactance must resonate out the receiver's self-reactance; and the optimal load resistance must balance the coupling co-

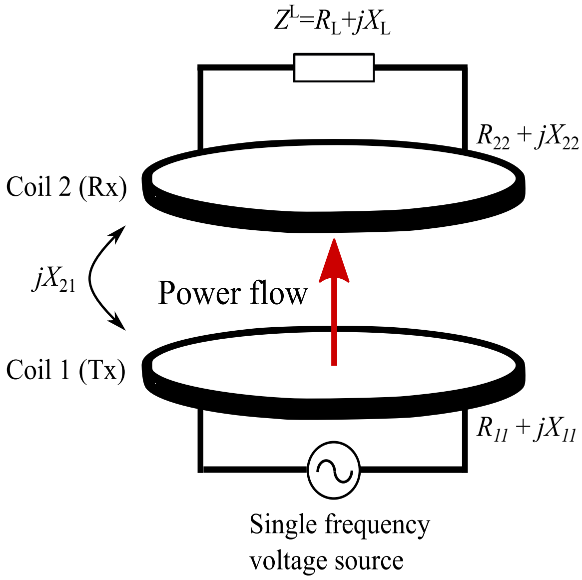

Figure 1.1: Single-receiver IPT system

efficient and the coil resistances. Achieved under this optimal condition, the maximum efficiency can be expressed in terms of an efficiency angle tangent coinciding with the square of kQ-product of the coils [7]. With all these achievements, the single-user IPT technique is reaching maturity.

First, we show about maximum transmission efficiency in single-receiver IPT system. Maximum efficiency in single-receiver IPT system, has been already studied by Mr. Ohira [7]. In below, we describe important points about maximum efficiency and kQ-product in the paper. Figure1.1 indicates the system of single-receiver IPT system. R_{11}, R_{22} and X_{11}, X_{22} are coil resistance and reactance of each coils respectively. Then, the X_{21} is mutual inductance between transmit coil and receiving coil. The resonance of the system is caused by the load reactance being added to the receiver so as to subtract the value of the reactance of the receiver. Then, we can obtain the maximum efficiency when the optimal load resistance"R_L" add to the receiver as shown below,

$$R_L = R_{22}\sqrt{1 + k^2Q^2}, \tag{1.1}$$

And maximum efficiency can be described as,

$$\eta_{max} = 1 - \frac{2}{1 + \sqrt{1 + k^2Q^2}} \tag{1.2}$$

As you can see, kQ-product is included in these equations. Here, k represents the coupling coefficient between the coils; and Q is the quality factor for each of them. Determined only by the configuration of the coil system, the maximum efficiency becomes an important performance indicator; and the optimal load, in its turns, guides the design process for loading and related conversion circuits.

1.2 Problem statement

In recent years, the multiple-receiver IPT system attracts great attention from many researchers [10]- [38]. The advantage of multi-receiver IPT is that it can supply power to each receiver simultaneously. However, when a single power transmiit coil feeds a plurality of receiving coils, the power received by each receiving coils fluctuates depending on the value of the load impedance of all the power receiving devices in the power feeding area, so that the power loss in the system design, it is important to know how much it is occurring. Therefore, the maximum efficiency of the entire system is an significant factor in developing multi-receiver IPT, and it is useful for development to know the relationship between the kQ-product and the maximum efficiency that was regarded as important in single-receiver IPT. However, unlike the single-receiver IPT system, the multiple-receiver IPT system is difficult to achieve the maximum efficiency due to cross-coupling among each receivers.

Recently, research attempts have been made to extend the concept of maximum efficiency and optimal load to system with multiple receivers. Optimization for multiple-receiver IPT link is quite challenging as it requires a joint optimization of resistances and reactances of multiple loads. Load resistances have been optimized in [15] under simplified assumptions, that there is no cross-coupling among receivers, and that each receiver applies individual resonance on its load reactance. However, in practice, the cross-coupling exists and may severely influence the system efficiency [16], necessitating a new criterion for deciding the load reactances rather than the individual resonance scheme. In order to compensate for the impact of cross-coupling, load reactances have been optimized separately with the load resistances for two receivers in [18] and for arbitrary number of receivers in [19]. For aforementioned the reasons, there is no case in load resistance and reactance has jointly optimized, and maximum efficiency has not mentioned perfectly, and that isn't inclueded the fields of resonance state. In this thesis, we achieve it by inserting an optimum load to each receiver. Also we clarify the effect of cross-coupling on efficiency and the relationship between maximum efficiency and kQ-product at the resonance state.

1.3 Contribution

The main contribution of this research is establishing a theory on load optimization and maximum efficiency of general multiple-receiver IPT system, serving as a criterion for the system design and benchmarking. To this end, we model the system and formulate the power transfer efficiency by using Z-parameters. Applying the first-order necessary condition, we derive the analytical formulas of optimal loads and maximum efficiency. We then perform full-wave 3D electromagnetic simulations, followed by experiments using vector network analyzar to validate the analytic results. Important conclusions are drawn as follows.

1. This validation clarifies interesting theoretical observation, that the load optimization perfectly mitigates the impact of cross-coupling, and that the maximum efficiency can also be expressed in terms of an efficiency angle tangent coinciding with the sum of squares of kQ-products of individual coupling links. The perspective enables maximum efficiency estimation of complicated multiple-receiver IPT system, at any scale, by measuring kQ-products of individual links, using a simple two-port network analyzer.

2. This observation implies that one can, in principle, increase the efficiency by increasing the number of receivers in case of the cross-coupling is mitigated parfectly.

3. This thesis also provides an extended analysis on system behavior at the optimal operating point, showing that the optimal load condition in fact reaches a resonance state.

1.4 Outline

The remainder of this thesis is organized as follows.

Chapter 2 introduces system model and summarizes theoretical results on maximum efficiency and further analyzes resonance state at the optimal load condition for experiment parts(Chapter 4). Next, Chapter 3 describes EM simuation system which is in various configuration, and shows that of result. Chapter 4 presents experiment method and the consequence in the two different case of receiving coils. Finally, Chapter 5 indicates conclusion and future works.

2 Theory on maximum achievable efficiency for multiple-receiver IPT systems

2.1 System model

A typical multiple-receiver IPT system is illustrated in Fig. 2.1, where coil $\#1$ is the single transmitter and coils $\#2$, $\#3$, $\ldots$, $\#N$ are the receivers. Coil $\#1$ is driven by a sinusoidal signal with frequency f and angular frequency $\omega = 2\pi f$. In the figure, r_1 and L_1 respectively represent the internal resistance and self-inductance of the transmit coil $\#1$; and M_{1n} or M_{n1} stands for the mutual-inductance between the transmit coil $\#1$ and the receive coil $\#n$ ($2 \leq n \leq N$). Similarly, r_n and L_n respectively denote the internal resistance and self-inductance of receive coil $\#n$; the mutual-inductance M_{nm} or M_{mn} between the coil $\#n$ and the coil $\#m$ ($2 \leq m \leq N$, $m \neq n$) models the cross-coupling between them. Using N-port network model, the relation between complex-valued phasors I_n of port-currents and phasors V_n of port-voltages V_n is expressed by (2.1).

$$\begin{bmatrix} V_1 \\ V_2 \\ \vdots \\ V_N \end{bmatrix} = \begin{bmatrix} r_1 + j\omega L_1 & j\omega M_{12} & \ldots & j\omega M_{1N} \\ j\omega M_{21} & r_2 + j\omega L_2 & \ldots & j\omega M_{2N} \\ \vdots & \vdots & \ddots & \vdots \\ j\omega M_{N1} & j\omega M_{N2} & \ldots & r_N + j\omega L_N \end{bmatrix} \begin{bmatrix} I_1 \\ I_2 \\ \vdots \\ I_N \end{bmatrix} \tag{2.1}$$

In this model, load impedance connected to the receive coil $\#n$ is represented by

$$Z_n^{\mathrm{L}} = R_n^{\mathrm{L}} + jX_n^{\mathrm{L}} = -V_n/I_n, \tag{2.2}$$

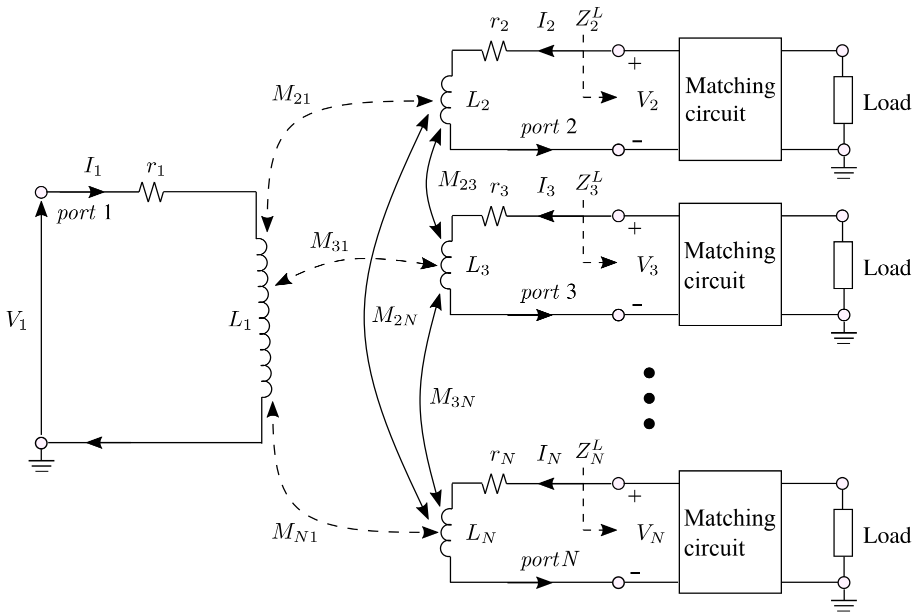

Figure 2.1: System model of multiple-receiver IPT system.

where $j = \sqrt{-1}$ is the imaginary unit. From (2.1), the RF power input to coil $\#1$ is straightforwardly defined by

$$\begin{aligned} P_{\text{in}} &= \frac{1}{2}\text{Re}\{V_1^* I_1\} \\ &= \frac{1}{2} r_1 |I_1|^2 - \frac{j\omega M_{n1}}{4} \sum_{n=2}^{N} (I_n^* I_1 - I_n I_1^*) \,. \end{aligned} \tag{2.3}$$

Here, $\text{R}e\{\cdot\}$ denotes the real part and $(\cdot)^*$ stands for the conjugate of a complex number. It is worth noticing that although (2.3) includes the imaginary unit j, the value of P_{in} is a real number because the term $(I_n^* I_1 - I_n I_1^*)$ is in fact equal to a purely imaginary value $j2\text{I}m\{I_n^* I_1\}$. Similarly, the output power from coil $\#n$ is $P_n = -\frac{1}{2}\text{R}e\{V_n^* I_n\}$, resulting in the total RF output power as follows.

$$\begin{aligned} P_{out} &= \sum_{n=2}^{N} P_n \\ &= -\frac{1}{2}\sum_{n=2}^{N} r_n |I_n|^2 - \frac{j\omega M_{n1}}{4} \sum_{n=2}^{N} (I_n^* I_1 + I_n I_1^*) \end{aligned} \tag{2.4}$$

Eventually, the system RF-to-RF efficiency is defined as

$$\eta = \frac{P_{out}}{P_{\text{in}}}. \tag{2.5}$$

2.1.1 Maximum achievable efficiency

Although (2.3) and (2.4) include I_1, efficiency η in fact depends on the relation between input current I_1 and output currents I_n. As a result, η can be viewed as a function of output currents I_n, taking I_1 as a parameter. Solving $\partial\eta/\partial I_n = 0$, we obtain the maximum efficiency

$$\eta_{\text{max}} = 1 - \frac{2}{1+\sqrt{1+\chi}}, \tag{2.6}$$

where χ is the so-called efficiency angle tangent given by

$$\chi = \sum_{n=2}^{N} \frac{\omega^2 M_{n1}^2}{r_1 r_n} = \sum_{n=2}^{N} \alpha_{n1}^2. \tag{2.7}$$

In (2.7), $\alpha_{n1}^2 = \omega^2 M_{n1}^2/(r_1 r_n)$ is the square of the kQ-product of the coupling between coil $\#1$ and coil $\#n$. As indicated in (2.6), the maximum efficiency of multiple-receiver scenario has the same form with that of the single-receiver case [12, 14]. The difference is the expression of the efficiency angle tangent χ. In single-receiver case ($n = 2$), $\chi = \omega^2 M_{n1}^2/(r_1 r_n)$, meaning that the efficiency angle tangent coincides with the kQ-product of the transmit and receive coils. In the multiple-receiver scenario, χ is the sum of squares of kQ-products of all individual couplings α_{n1}^2. Interestingly, the expressions of χ in this case does not include the mutual-inductance M_{nm} between any two receive coils, meaning that the load optimization completely mitigate the impact of cross-coupling. The relation between maximum efficiencies of single-receiver and multiple-receiver systems is illustrated in Fig. 2.2. In the figure, the curve demonstrates η_{max} as a function of χ. The efficiency of single-receiver system, e.g., the system of coil $\#1$ and coil $\#2$ can be predicted by projecting the corresponding α_{21}^2 into the curve. The value of χ for the multiple-receiver system is obtained by summing up all individual α_{n1}^2. Efficiency of the multiple-receiver system is then obtained by projecting χ into the curve. As a result, efficiency evaluation for SIMO systems at any scale can be conducted by using a simple two-port network analyzer to measure kQ-products of each individual link.

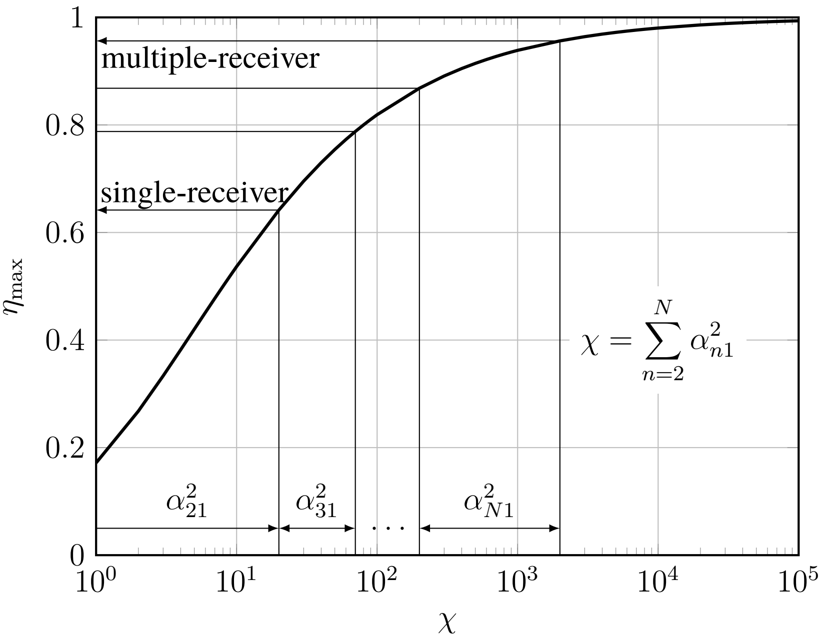

Figure 2.2: Relation between maximum efficiencies of single-receiver and multiple-receiver IPT systems.

At the optimal operation point, the input and output currents satisfy the relation below.

$$I_n^{(opt)} = -j\frac{\omega M_{n1}(1-\eta_{\max})}{2r_n}I_1. \tag{2.8}$$

As a result, the optimal loads for achieving the maximum efficiency is

$$R_n^{\mathrm{L}(opt)} = r_n\sqrt{1+\chi}, \tag{2.9}$$

$$X_n^{\mathrm{L}(opt)} = -\omega L_n - \omega\sum_{\substack{m=2\\m\neq n}}^{N} M_{nm}\frac{M_{m1}r_n}{M_{n1}r_m}. \tag{2.10}$$

The optimal resistance for the receive coil $\#n$ depends on its internal resistance and the efficiency angle tangent, which is determined by the coil configuration. The optimal reactance depends on the self-reactance of the coil $\#n$, internal resistances and mutual coupling among all the other coils in the system. Therefore, the optimal loads for achieving the maximum efficiency basically vary with the configuration and arrangement of the coils.

Under the optimal load condition the ratio of output power at receiver $\#n$ to the total output power is given by

$$\gamma_n = \frac{P_n^{(opt)}}{P_{\text{out}}^{(opt)}} = \frac{\alpha_{n1}^2}{\sum_{n'=2}^{N} \alpha_{n'1}^2}. \tag{2.11}$$

As shown in (2.11), the output power ratio depends on the square of kQ-product of the link between the transmit coil and the receive coil $\#n$, meaning that different receivers might obtain different power levels according to coil arrangement.

2.1.2 Resonance at optimal load condition

In this section, we describe the resonance under optimal load condition for Chapter.4 The optimal load condition mentioned above is in fact at a resonance state. To clarify this observation, let us consider series impedance Z_n^{all} of all elements in the receive coil $\#n$. From (2.1) and (2.2), it follows

$$\begin{aligned} Z_n^{\text{all}} = r_n + R_n^{\text{L}(opt)} &- \overbrace{j\omega \textstyle\sum_{\substack{m=2 \\ m\neq n}}^{N} M_{nm} \frac{I_m}{I_n}}^{parasitic\ impedance} \\ &+ \underbrace{j\omega \textstyle\sum_{\substack{m=2 \\ m\neq n}}^{N} M_{nm} \frac{M_{m1} r_n}{M_{n1} r_m}}_{compensatory\ reactance} \end{aligned} \tag{2.12}$$

In (2.12), the third term is the parasitic impedance induced by cross-coupling with other receive coils; and the fourth term is the compensatory reactance of the optimal load. The parasitic impedance depends on the relation between output currents I_2, ..., I_N. At the optimal load condition, the output currents satisfy condition (2.8), resulting in a complete cancellation of the parasitic component by the compensatory reactance. As a result, the series impedance of all elements is purely resistive

$$Z_n^{\text{all}(opt)} = r_n + R_n^{\text{L}(opt)}. \tag{2.13}$$

On the other hand, if all the receivers follow the common practice of resonating out their self-rectances individually, the load reactance for coil $\#n$ is $X_n^{\text{L}(conv)} = -\omega L_n$. In such a case, as the compensatory rectance does not exit, the parasitic impedance still remains in the series impedance of all elements as follows.

$$Z_n^{\text{all}(conv)} = r_n + R_n^{\text{L}(opt)} - \underbrace{j\omega \textstyle\sum_{\substack{m=2 \\ m\neq n}}^{N} M_{nm} \frac{I_m}{I_n}}_{parasitic\ impedance}. \tag{2.14}$$

Due to many possible values of the output current set I_n, the parasitic impedance in (2.14) might include both resistive and imaginary components. Since all the receive coils are passive elements, this resistive component must take positive values, meaning that $\left|Z_n^{\mathrm{all}(conv)}\right| \geq Z_n^{\mathrm{all}(conv)}$ for all possible values of the output current set. This proves that $Z_n^{\mathrm{all}(opt)}$ is the minimum of $\left|Z_n^{\mathrm{all}}\right|$ and indicates that all the receive coils simultaneously resonate at the optimal load condition.

3 Computer simulation and analysis

3.1 EM Simulation

In this section, we investigate the efficiency and squares of kQ-product characteristics of various multi-receiver configurations. In the simulation, we use single turn circular coil for transmitter and receivers which are made from copper wire with diameter of 1mm and with conductivity of 5.8×10^7S/m. The radii of all coils are constantly 150mm. Operating frequency f=13.56MHz. The distance from transmitter is denoted by d[mm]. The efficiency η is plotted by d $(0 \leq d \leq 275)$ which is at interval at 25mm. In the following investigation, we compare efficiency and of two schemes. The "Joint-opt." scheme in which load resistances and reactances are jointly optimized by (2.9) and (2.10). The "Local-opt." scheme in which only load resistances are optimized following (2.9) and the impact of cross-coupling is considered. For reference, we also add the curve "Theory (2.6)", in which the efficiency is directly calculated by 2.6. In this regard, the agreement between the "Joint-opt." and "Theory 2.6" curves indicate the optimality of the derived solution. The gap between the "Joint-opt." and "Local-opt." curves demonstrate the impact of cross-coupling. In those schemes, we also caluculate their squares of kQ-product is given by efficiency of "Joint-opt" scheme. And then, we show that the squares of kQ-product in optimized system matches the sum of squares of kQ-products of individual transmitter-receiver links [13]. Therefore, we compare the squares of kQ-product in optimized system matches the sum of kQ-products is given by system model.

3.1.1 Coplanar arrangement

In this case, the position of receivers is symmetrical about transmitter, the cross-coupling among receivers is almost constant as we vary the value of d. As shown in

Table 3.1: Simulation paramters(Coplanar, Coaxial).

Parameters	Value
Operating fequency	$13.56[MHz]$
Coils raii	$150[mm]$
Conductivy	$5.8 \times 10^7[S/m]$
Copper wire dianeter	$1.0[mm]$
Airgap d	$25 - 275[mm]$
Coil resistance and reactance	$0.24 + j93.0[\Omega]$
Analysis	$moment\ method(MoM)$

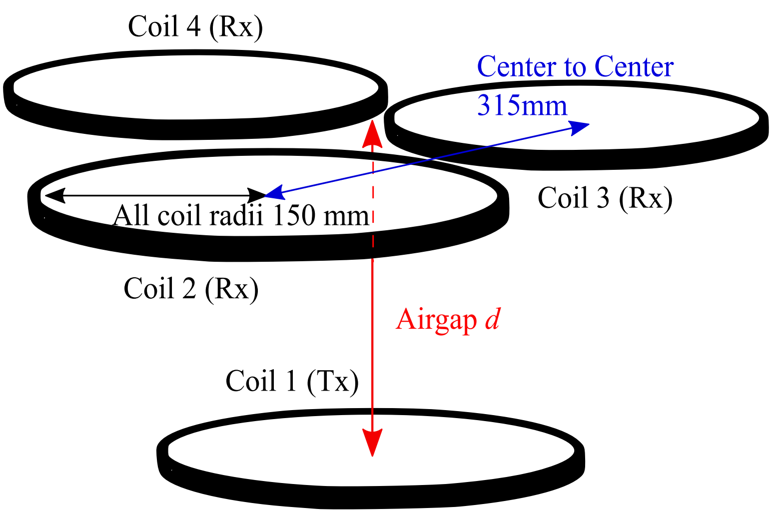

Figure 3.1: Coplanar three-receiver system

Fig. 3.1, three-receiver coils are placed in same plane, and the center of them is around 312mm away from each other.

From Fig. 3.2, it can be seen that theoretical maximum efficiency is achieved if load resistances and reactances are jointly optimized. The impact of cross-coupling becomes more severe as the distance is increasing, for example, the performance gap is around 40% at d=275[mm]. This is because the coupling between transmitter and receivers become weaker as distance d increases.

Fig. 3.3, the squares of system kQ-product matches the sum of squares of kQ-

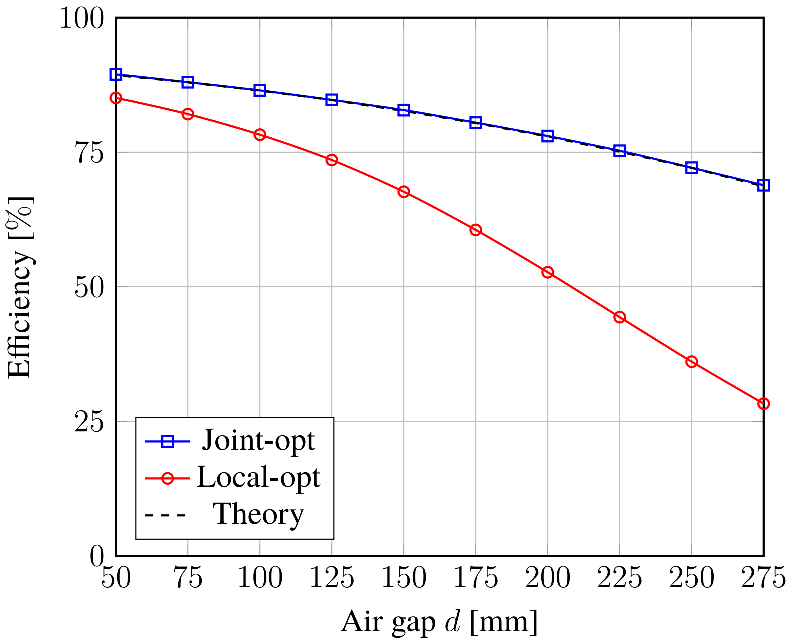

Figure 3.2: Efficiency performance of system in Fig. 3.1

products of individual transmitter-receiver links.

3.1.2 Coaxial arrangement

In this case, the position of receivers is on same axis of transmitter, and distance among receivers is 25mm each other, like Fig. 3.4

From Fig. 3.5 and Fig. 3.6, The characteristics are similar to those of Fig. 3.2 and Fig. 3.3, respectively. The difference from Fig. 3.2 and Fig. 3.5, is that the impact of cross-coupling in Fig. 3.5 become more drastic than that in Fig. 3.2. This is because the cross-coupling among receivers in Fig. 3.4, is stronger than that of Fig. 3.1. The maximum improvement is around 75% at d=275[mm]. Figure. 3.6 indicates that the system kQ-product is equal to sum of individual links, verifying the effectiveness of (2.7).

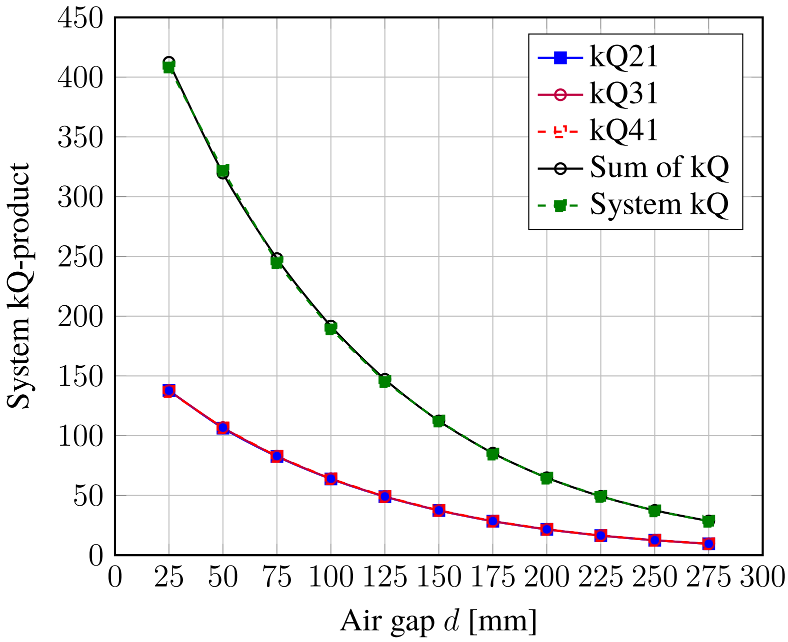

Figure 3.3: Efficiency performance of system in Fig. 3.1

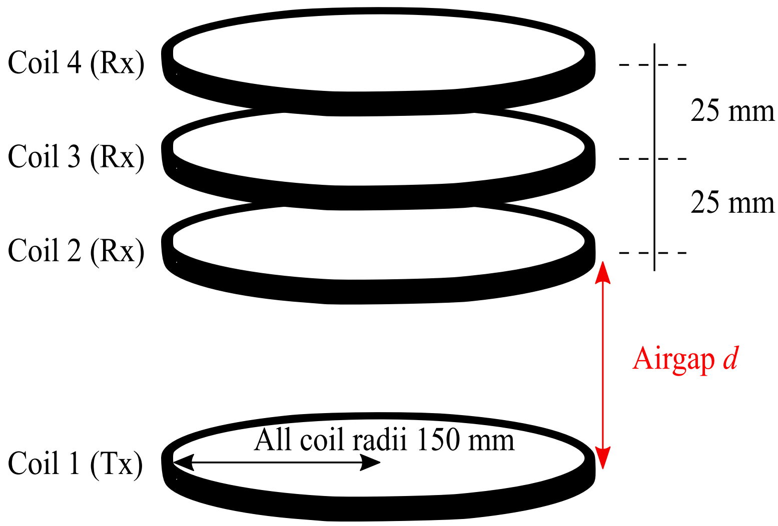

Figure 3.4: Coaxial three-receiver system

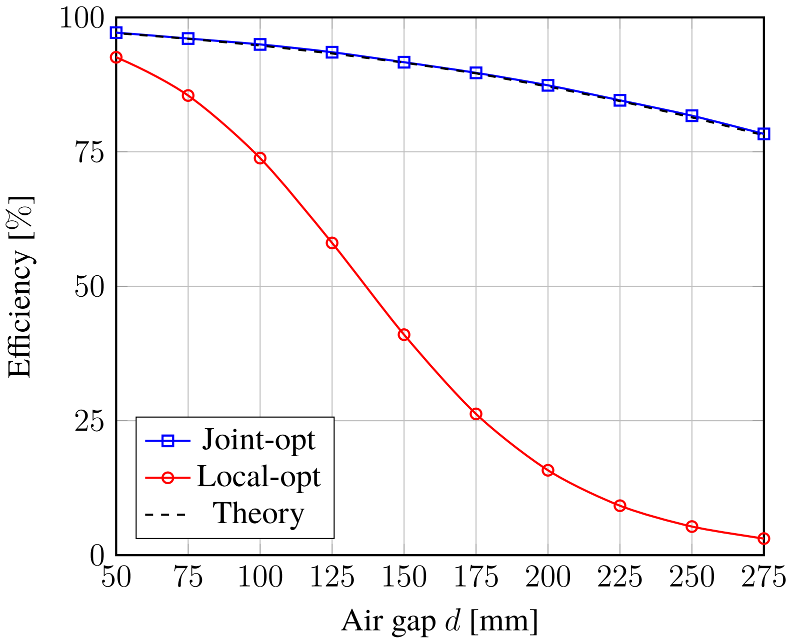

Figure 3.5: Efficiency performance of system in Fig. 3.1

3.1.3 Coaxial multiple-receiver system

We analyze maximum efficiency for IPT system with many receivers. However, in simulation, the more number of receivers increases, the time of simulation becomes longer. Therefore, we set the maximal number of receivers is six to analyze the characteristic of arbitrary number of receivers. All receiving coils $n \in \{2, \ldots, 6\}$ are placed on the same axis with transmitter coil as described in Fig. 3.7. The distance of between receiving coils is 25mm. Figure. 3.8, further confirms the performance characteristics in Fig. 3.1 and Fig. 3.5.

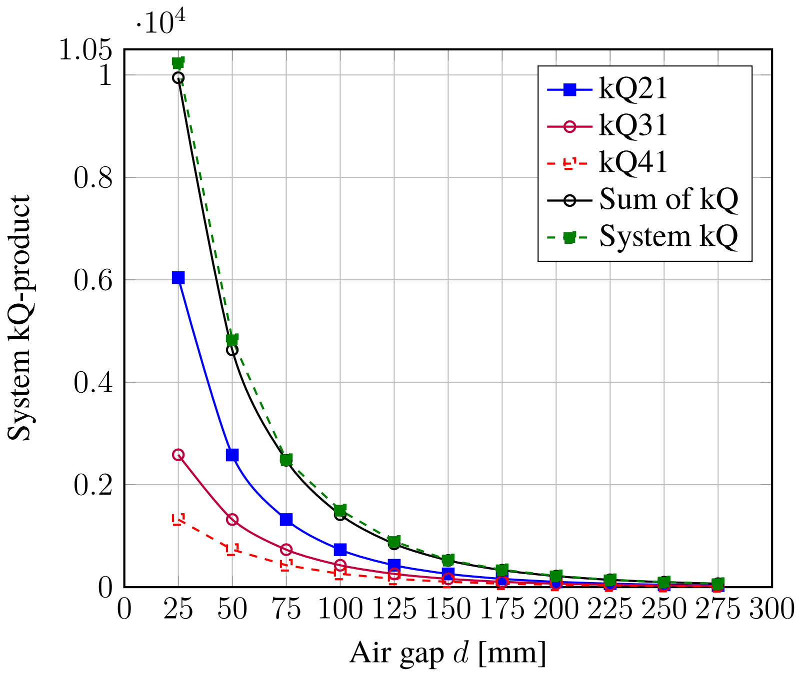

Figure 3.6: Efficiency performance of system in Fig. 3.1

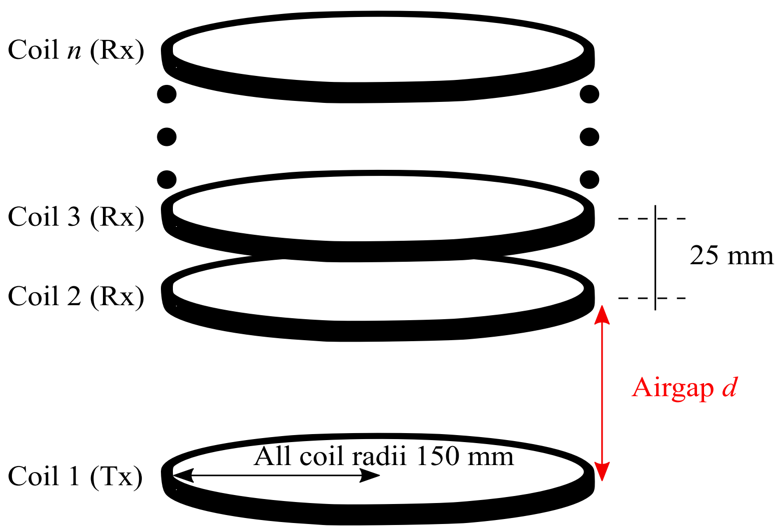

Figure 3.7: Coaxial multiple-receiver system

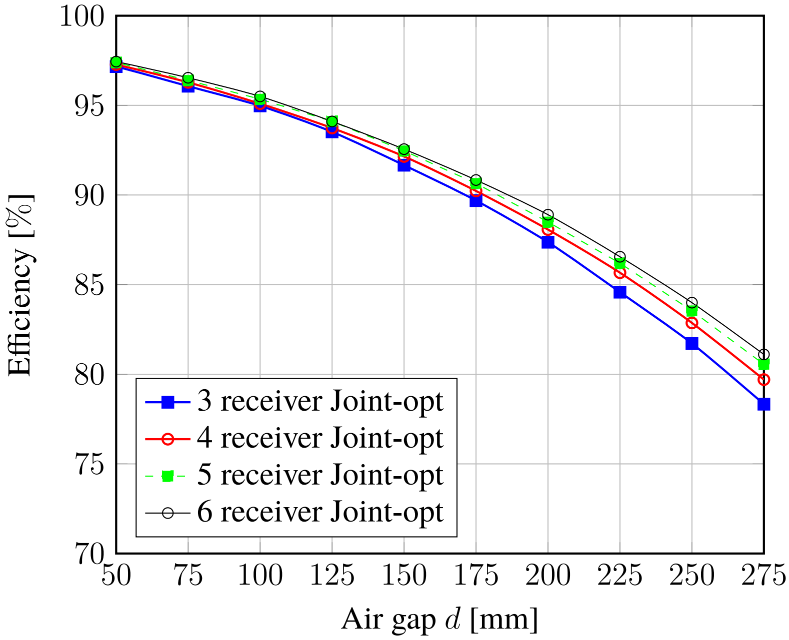

Figure 3.8: Efficiency performance of system in Fig. 3.1

4 Experimental Evaluation

4.1 Experiment setup

We validate the theory in Chapter.2 by comparing three values of the maximum efficiency: (1) theoretical, (2) experimental and (3) simulation values. Experimental setup and detail measurements for each values are described below.

1. The theoretical value is obtained by directly substituting the equivalent circuit parameters in (2.1) into (2.6). The parameters are obtained by measurement using network analyzer (VNA). In this paper, we use a four-port ADVANTEST® VNA R3767CG with reference impedance $z_0 = 50\ \Omega$ for all ports. From the measured parameters, the theoretical value of output power ratio in (2.11) is also calculated.

2. The experimental value is the efficiency achieved at the optimal load condition. To measure this value, it is necessary to adjust the port impedances of the VNA to the optimal loads. A straightforward method is to fabricate matching networks and insert them between the IPT system and the VNA ports. However, this method is time-consuming and inaccurate due to losses in the matching networks. In order to facilitate the measurement process, we exploit the software fixture function in the VNA to transform the port impedances in a software-based manner. It should be clarified that the software fixture function does not physically change the port impedances but only modifies and displays the measurements, as if the port impedances have been adjusted to the target values. As the losses and the hassle fabrication of matching networks are removed, this method is capable of accurate evaluation for various coil settings, enabling concrete validation for the theory. To be specific, a virtual L-match shown Fig. 4.1 is used to convert the port impedance $z_0 = 50\ \Omega$ to optimal loads $Z_n^{\mathrm{L}(opt)}$ with the capacitor C_n^{M} and the inductor L_n^{M} are

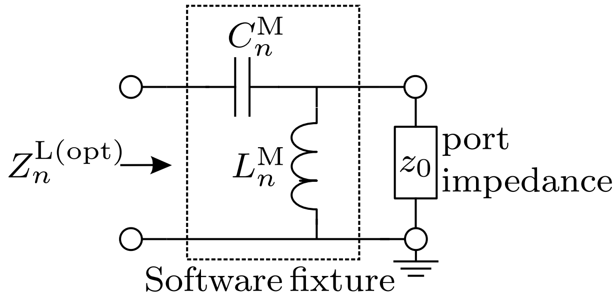

Figure 4.1: Virtual port impedance transform by software fixture function.

initially determined as

$$L_n^{\mathrm{M}} = \sqrt{\frac{z_0^2 R_n^{\mathrm{L}(opt)}}{\omega^2 (z_0 - R_n^{\mathrm{L}(opt)})}}. \tag{4.1}$$

$$C_n^{\mathrm{M}} = \left(\frac{z_0^2 \omega^2 L_n^{\mathrm{M}}}{z_0^2 + \omega^2 L_n^{\mathrm{M}}} - \omega X_n^{\mathrm{L}(opt)} \right)^{-1}, \tag{4.2}$$

Due to uncertainties in the VNA, these values are insufficient to yield the required load impedances. Therefore, we have also performed fine adjustment on C_n^{M} and L_n^{M} in order to reduce errors. After this adjustment, we measure S-parameters $|S_{11}^{(opt)}|$ and $|S_{n1}^{(opt)}|$ at the optimal load condition and calculate the achieved efficiency following the equation below

$$\eta^{exp} = \frac{\sum_{n=2}^{N} |S_{n1}^{(opt)}|^2}{1 - |S_{11}^{(opt)}|^2}. \tag{4.3}$$

In addition, the experimental value of output power ratio is also calculated by

$$\gamma_n^{exp} = \frac{|S_{n1}^{(opt)}|^2}{\sum_{n'=2}^{N} |S_{n'1}^{(opt)}|^2}. \tag{4.4}$$

3. The simulation value is the efficiency obtained at the optimal load condition when performing EM simulation on the same coil configurations and arrangements with those in the experiments. All EM simulations are based on the MoM. In the simulations, we have also added additional resistances to the coils to compensate for parasitic resistances and contact resistances in experiments.

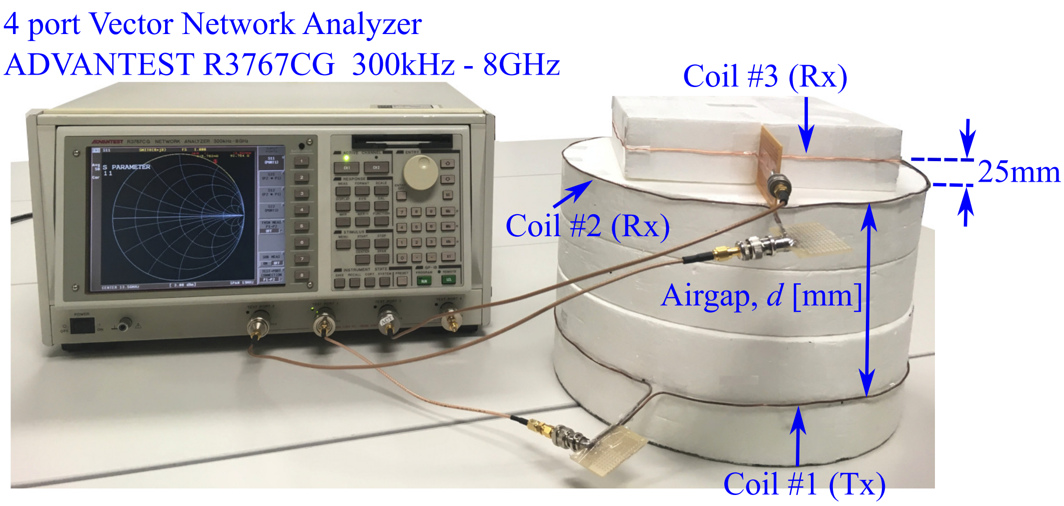

Figure 4.2: Experiment setup of two-receiver system.

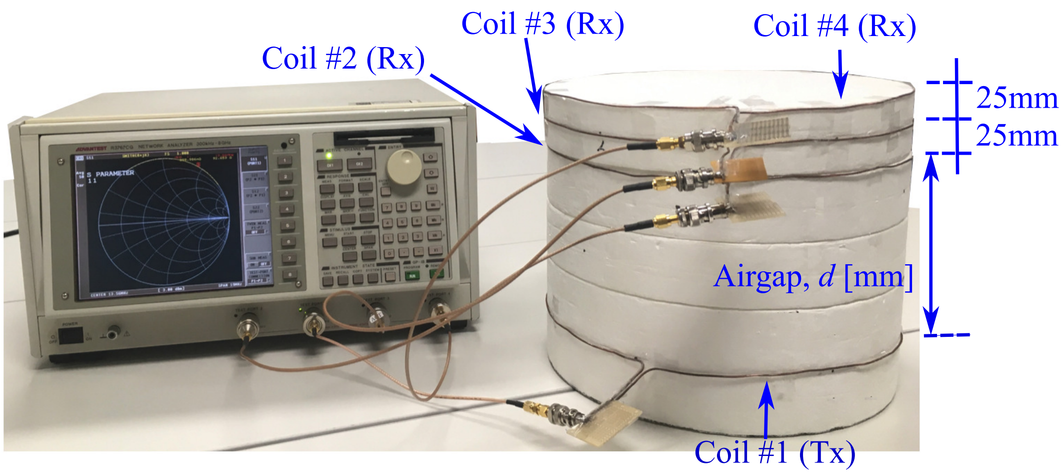

Figure 4.3: Experiment setup of three-receiver system.

The aforementioned three values will be measured for two-receiver system in Fig. 4.2 and three-receiver in Fig. 4.3 as the four-port VNA R3767CG only allows measurements for configurations of up to three receivers. In these two configurations, all the coils are single-turn coil made of copper wire (conductivity 5.8×10^7 S/m) with diameter 1.5

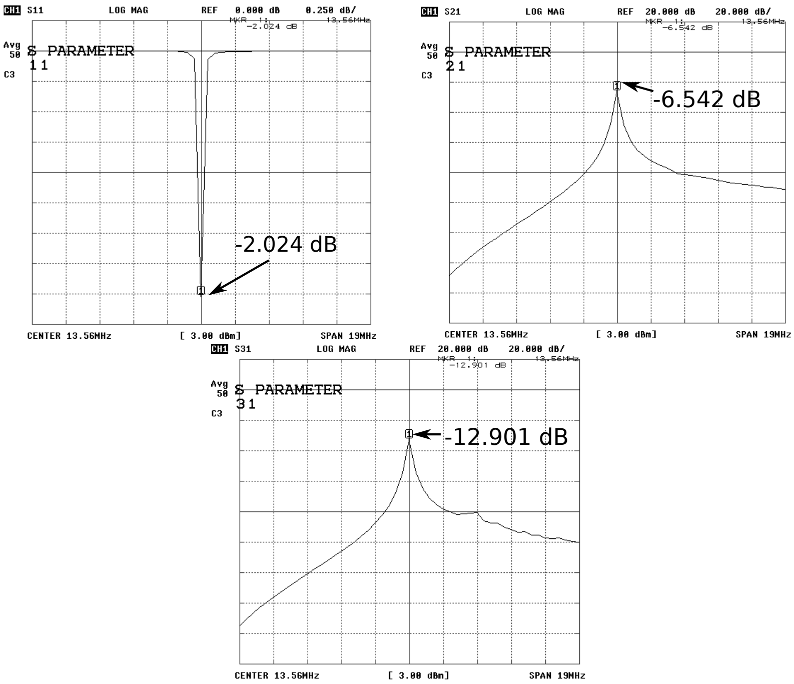

Figure 4.4: S-parameters at optimal load condition for two-receiver system with $d = 350$ mm.

mm. We use two types of coils: circular coil and square coil. The circular coils have identical diameters of 300 mm; and the square coil dimensions are 200 mm$\times$200 mm. In each of the systems, all coils are placed coaxially in order to introduce cross-coupling among receivers. The distances between any two adjacent receivers are kept constant at 25 mm while the distance d from the transmitter to the group of receivers is varied. The operation frequency is set to $f = 13.56$ MHz.

4.2 Results

4.2.1 Two-receiver system

First, we consider the two-receiver system in Fig. 4.2 with the distance $d = 350$ mm. With this configuration, the measurements of system parameters are shown in Table 4.1. In the table, it is obvious that M_{32} (or M_{23}) is significant compared to M_{21} and M_{31}, meaning that there is cross-coupling between the two receivers. From the parameters,

Table 4.1: Measured parameters of two-receiver system in Fig. 4.2 with $d = 350$ mm.

r_1	0.2 Ω	L_1	1244 nH	$M_{12} = M_{21}$	15 nH
r_2	0.3 Ω	L_2	1279 nH	$M_{13} = M_{21}$	8 nH
r_3	0.3 Ω	L_3	950 nH	$M_{23} = M_{32}$	203 nH

we obtain a theoretical maximum efficiency of 71.0$\%$ by applying (2.6). The optimal loads are then calculated by using (2.9) and (2.10), resulting in $Z_2^{\mathrm{L}(opt)} = 1.9 - j117.0$ Ω and $Z_3^{\mathrm{L}(opt)} = 1.9 - j115.0$ Ω. We then adjust the virtual L-match in software fixture so that the port impedances reach these values. Frequency characteristics of the S-parameters at this optimal condition are then observed as in Fig. 4.4. As shown in this figure, at the frequency of interest of 13.56 MHz, the magnitude of S_{11} becomes minimum while those of S_{21} and S_{31} reach their maxima. This verifies that the system reaches a resonance state when the optimal load condition is applied. Substituting the magnitudes of S_{11}, S_{21} and S_{31} at 13.56 MHz into (4.3), we obtain the experimental value for efficiency is 70.1$\%$. Carrying out EM simulation for the same configuration, we get a simulated efficiency is 70.4$\%$. Here, it is clear that theory, experiment and simulation results are very close to each other.

The aforementioned process is then repeated for other values of the distance d. Figure 4.5 plots approximate curves of efficiencies which are obtained via theory, experiment and simulation. As is demonstrated in the figure, the three lines are very tight to each other. It can be observed that when d is at around 200 mm, the difference between the three values becomes largest. However, even at with this configuration, the difference between simulation and theory results is only 4.2$\%$; and the difference between simulation and experiment results is only 0.8$\%$. This validates the formulas of maximum efficiency and optimal loads in (2.6), (2.9) and (2.10).

Output power ratio for receive coils 2$\#$ and $\#$3 are shown in Fig. 4.6. As is evident in the figure, the experiment result agrees very well with the theoretical formula in (2.11). Furthermore, the figure also demonstrates that coil $\#$2 receives a higher power than coil $\#$3. As shown in the coil configuration of Fig. 4.2, because coil $\#$2 is larger than and closer to the transmitter, it has a higher kQ-product, and consequently, receives a higher power than coil $\#$3.

Table 4.2 presents optimal loads for achieving maximum efficiency for various values

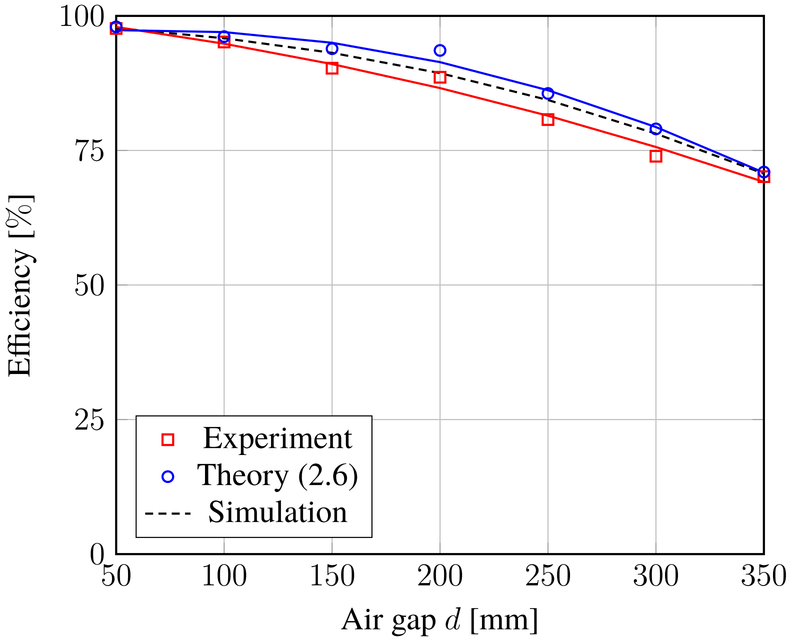

Figure 4.5: Efficiency evaluation for two-receiver system in Fig. 4.2.

Table 4.2: Optimal loads for two-receiver system in Fig. 4.2

d [mm]	$Z_2^{\mathrm{L}(opt)}$ [Ω]	$Z_3^{\mathrm{L}(opt)}$ [Ω]
50	$31.5 - j117.1$	$31.6 - j121.1$
100	$16.6 - j117.9$	$16.6 - j118.2$
150	$10.3 - j117.9$	$10.3 - j117.7$
200	$9.8 - j118.0$	$9.8 - j117.6$
250	$4.2 - j118.0$	$4.2 - j117.6$
300	$2.8 - j118.0$	$2.8 - j117.8$
350	$1.9 - j117.2$	$1.9 - j115.1$

of d. The table implies that the optimal loads are realizable in practice but need to be adaptively updated with the distance d.

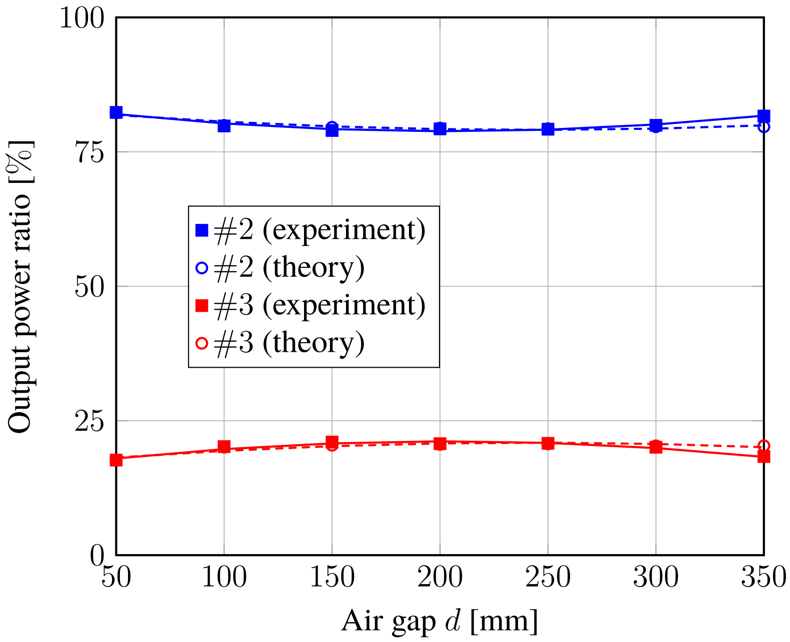

Figure 4.6: Efficiency angle tangent for two-receiver system in Fig. 4.6.

4.2.2 Three-receiver system

Figure 4.7 demonstrates the frequency characteristic of S-parameters for the three-receiver system in Fig. 5 with the distance $d = 350$ mm. Similar to the result in Fig. 4.4, at the tuned frequency of 13.56 MHz, the magnitude of S_{11} becomes minimum while those of S_{21}, S_{31} and S_{41} reach their maxima. This result confirms gain that the system is at a resonance state in the optimal load condition.

Figure 4.8 shows the theoretical, experimental and simulation values of the maximum efficiency for the three-receiver system in Fig. 4.9 with various values of d. The good agreement between the three values shown in this figure validates the formulas of maximum efficiency and optimal loads. Figure 4.9 demonstrates that the experiment results of output power ratio agree well with the theoretical formula in (2.11) for the three-receiver system. Table 4.3 indicates again that the optimal loads are realizable but need to be adaptively updated with the coil arrangement.

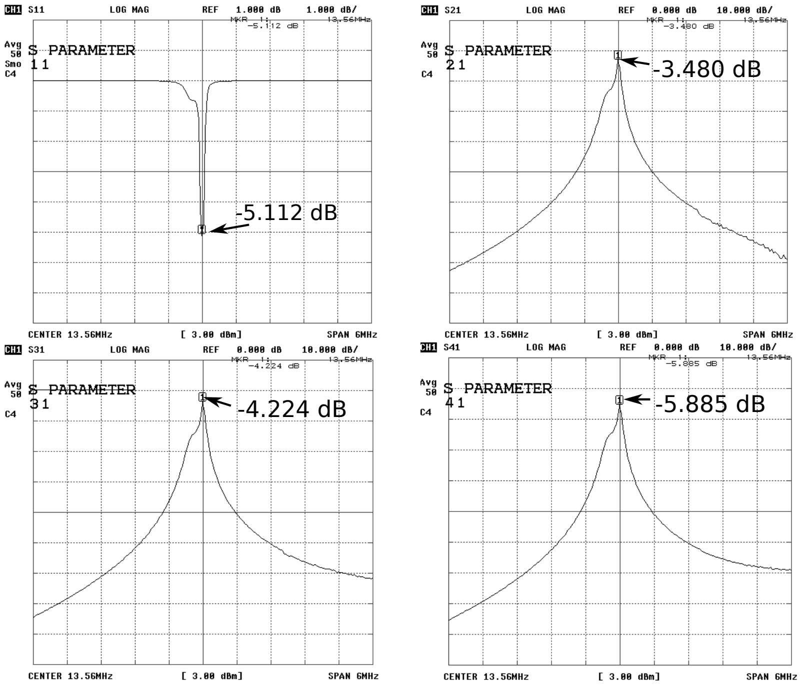

Figure 4.7: S-parameters at optimal load condition for three-receiver system with $d =$ 350 mm.

Table 4.3: Optimal loads for three-receiver system in Fig. 4.3

d [mm]	$Z_2^{\mathrm{L}(opt)}$ [Ω]	$Z_3^{\mathrm{L}(opt)}$ [Ω]	$Z_4^{\mathrm{L}(opt)}$ [Ω]
50	$30.0 - j128.9$	$22.8 - j149.3$	$31.0 - j173.6$
100	$18.3 - j128.0$	$13.9 - j151.2$	$18.9 - j170.1$
150	$10.0 - j132.9$	$7.63 - j146.8$	$10.3 - j165.3$
200	$5.9 - j133.0$	$4.5 - j145.2$	$6.1 - j165.0$
250	$3.8 - j134.0$	$2.9 - j144.2$	$4.0 - j160.9$
300	$2.7 - j136.6$	$2.1 - j143.1$	$2.8 - j166.0$
350	$2.0 - j135.8$	$1.5 - j143.3$	$2.0 - j160.7$

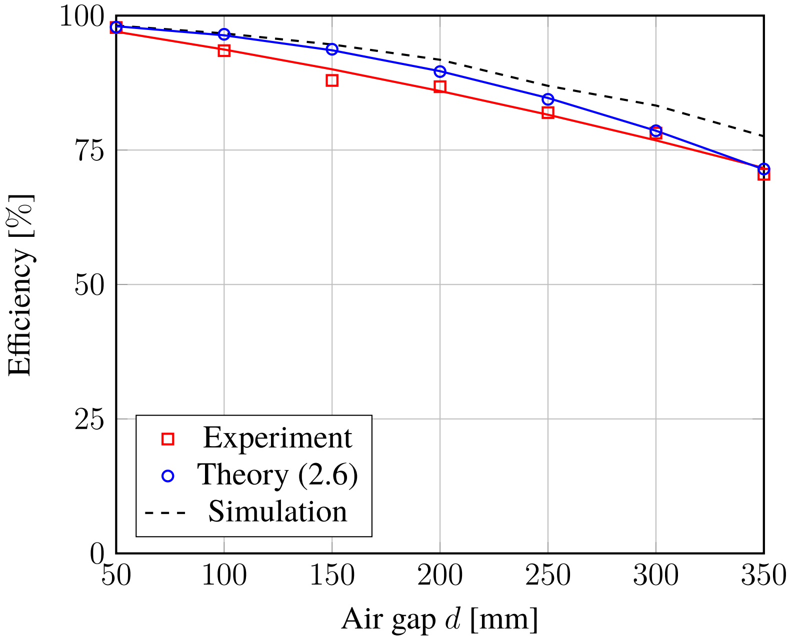

Figure 4.8: Efficiency evaluation for three-receive system in Fig. 4.3.

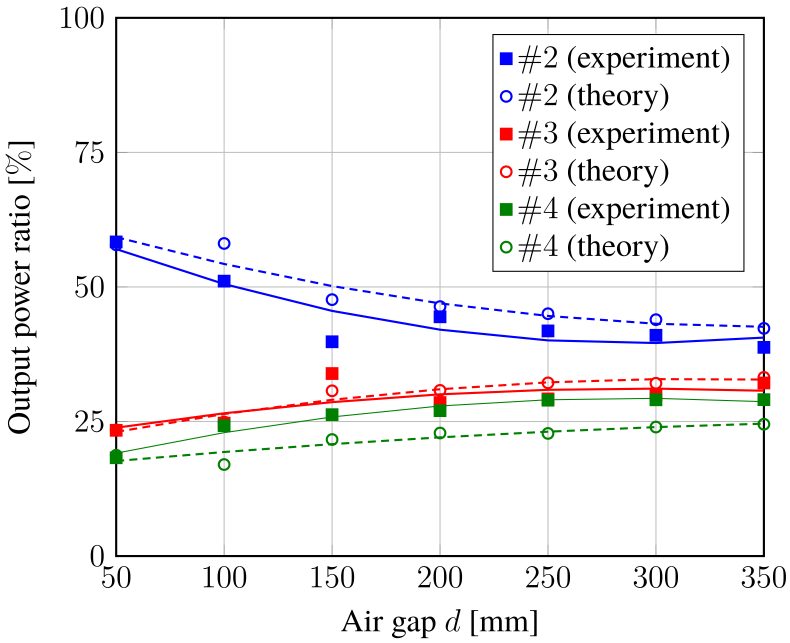

Figure 4.9: Efficiency angle tangent for three-receiver system in Fig. 4.3.

5 Conclusion

In this thesis, we analyzed maximum achievable efficiency of IPT system with arbitrary number of receivers focusing on the cross-coupling effect. First, we model the system and express the relation of current-voltage by Z-parameter, formulating power transmission efficiency. Next, applying the first-order necessary condition, we derive the analytical formulas of optimal loads and maximum efficiency. Finally, We then perform full-wave 3D electromagnetic simulations, followed by experiments using vector network analyzar to validate the analytic results. In order to validate the maximum efficiency formulation, this thesis has presented extended analysis and S-parameter evaluation on the behaviors of multiple-receiver IPT system at the optimal load condition. Specifically, we showed that, the cross-coupling among receivers does not affect system efficiency if load resistances and reactances are jointly optimized. We also analytically proved that maximum efficiency is dominated by a system kQ-product, whose square is equal to sum of squares of kQ-products of individual transmitter-receiver links. In other wards, the system is in a resonance state; the efficiency reaches its maximum expressed by an efficiency angle tangent coinciding with sum of squares of kQ-products of individual links, in an manner analogous to the well-known kQ-theory for single-receiver IPT. This observation implies that one can, in principle, increase the efficiency by increasing the number of receivers, and it enables efficiency estimation of complicated multiple-receiver IPT system at any scale by using a simple vector network analyzer with two port.

Acknowledgements

In the begining, I would like to thank Proffesor Minoru Okada for leading me to this grdauate school and warmly welcoming it to the laboratory. From day-to-day he cared about my condition because I often stayed being at late night in my lab. His kindness and advice gave me a motivation to study hard. Also, I would like to express my thanks to all professors in my lab. Beside meeting, they made time to discuss with me and provided me with useful advice from their knowledge and experience: Associate Proffessor Higashino Takeshi and remarkably Assistant Proffesor Duong Quang Thang. He did carefully supervise me many times, and he gave me two chances to join international conference, and they are special experience for me. And, I want to express my thanks to Proffesor Sugimoto Kenji from the Intelligent System Controk laboratory for his help about improving the quality of my master thesis. I also thank you Professor Kosin Kosin Chamnongthai for giving me an oppotunity to join King Mongkut's University of Technology Thonburi (KMUTT) short-term internship. During the internship period, many KMUTT students taught me the culture of Thailand and they are very hospitable to us. Especially, I would like to express my gratitude to NOW. She gave me medicines while I was sick, and she rescued me many times because I do not understand Thai. Thank to all the Network System lablatory members, I enjoyed having fun every day. Thank you all my freinds. I received a good stimulation from them. Finally, Thank you my family. I was able to spend peace of mind because my family supported me.

References

[1] Andre Kurs, Aristeidis Karalis and Robert Moffatt *et al.*, "Wireless Power Transfer via Strongly Coupled Magnetic Resonances," Science., vol. 317, issue 5834, pp. 83-86, 06 Jul 2007.

[2] "OECD Policy Guidance on Radio Frequency Identification", https://www.oecd.org/sti/ieconomy/40892347.pdf (Accessed on 01/26/2018)

[3] Manuel Pinuela, David C. Yates, Stepan Lucyszyn and Paul D. Mitcheson, "Maximising DC to Load Efficiency for Inductive Power Transfer," IEEE Transactions on Power Electronics, 28(5):2437-2447, May 2013 (DOI: 10.1109/TPEL.2012.2215887)

[4] G. A. Covic and J. T. Boys, "Modern Trends in Inductive Power Transfer for Transportation Applications," IEEE Journal of Emerging and Selected Topics in Power Electronics, vol.1, No.1, Mar 2013. (DOI: 10.1109/JESTPE.2013.2264473)

[5] "Wireless Charging Market Size By Application, By Technology, Industry Analysis Report, Regional Outlook, Application Potential, Price Trends, Competitive Market Share & Forecast, 2017 – 2024," https://www.gminsights.com/industry-analysis/wireless-charging-market (Accessed on 01/27/2018)

[6] "Trends, Technical and Regulatory Problems, and Standardization for Commercialization of Wireless Power Transmission Technologies," http://www.cic-infonet.jp/section/activity/pdf/121207_2.pdf (Accessed on 01/27/2018)

[7] T. Ohira, "Extended k-Q product formulas for capacitive- and inductive-coupling wireless power transfer schemes," IEICE Electron. Express, vol. 11, no. 9, pp. 1–7, Apr. 2014.

[8] “wireless power transfer system for EV,” http://www.daihen.co.jp/products/wireless/ev/ (Accessed on 01/20/2018).

[9] Hybrid - EV Commitee “Wireless Power Transfer for Light-Duty Plug-In / Electric Vehicles and Alignment Methodology” published J2954 on May 31, 2016 https://www.sae.org/standards/content/j2954_201605/ (Accessed on 01/25/2018).

[10] G. A. Covic and J. T. Boys, “Inductive power transfer,” Proceedings of the IEEE, vol. 101, no. 6, pp. 1276–1289, June 2013.

[11] T. Imura and Y. Hori, “Maximizing air gap and efficiency of magnetic resonant coupling for wireless power transfer using equivalent circuit and Neumann formula,” IEEE Trans. Ind. Electron., vol. 58, no. 10, pp. 4746–4752, Oct. 2011.

[12] M. Zargham and P. G. Gulak, “Maximum achievable efficiency in near-field coupled power-transfer systems,” IEEE Trans. Biomed. Circuits Syst., vol. 6, no. 3, pp. 228–245, June 2012.

[13] T. Ohira, “Angular expression of maximum power transfer efficiency in reciprocal two-port systems,” in Proc. IEEE Wireless Power Transf. Conf., South Korea, Jeju, May 2014.

[14] T. Ohira, “Maximum available efficiency formulation based on a black-box model of linear two-port power transfer systems,” IEICE Electron. Express, vol. 11, no. 13, pp. 1–6, July 2014.

[15] M. Fu, T. Zhang, C. Ma and X. Zhu, “Efficiency and optimal loads analysis for multiple-receiver wireless power transfer systems,” IEEE Trans. Microw. Theory Techn., vol. 63, no. 3, pp. 801–812, Feb. 2015.

[16] D. Ahn and S. Hong, “Effect of coupling between multiple transmitters or multiple receivers on wireless power transfer,” IEEE Trans. Ind. Electron., vol. 60, no. 7, pp. 2602–2613, July 2013.

[17] T. Imura, “Cross-coupling canceling method for wireless power transfer via magnetic resonance coupling," IEEJ Trans. Ind. Applicat., vol. 134, no. 5, pp. 564–574, 2014 (in Japanese).

[18] C. Zhong, B. Luo, F. Ning and W. Liu, “Reactance compensation method to eliminate cross coupling for two-receiver wireless power transfer system,” IEICE Electron. Express, vol. 12, no. 7, pp. 1–7, Apr. 2015.

[19] M. Fu, T. Zhang, X. Zhu, P.C. Luk and C. Ma, “Compensation of cross coupling in multiple-receiver wireless power transfer systems,” IEEE Trans. Ind. Informat., vol. 12, no. 2, pp. 474–482, Apr. 2016.

[20] T. Zhang *et al.*, “Optimal load analysis for a two-receiver wireless power transfer system,” 2014 IEEE wireless power transfer Conf (WPTC), Jeju, May, 2014, pp. 84-87.

[21] T. Imura, “Simultaneous wireless power transfer via magnetic resonant coupling to multiple receiving coils,” IEEJ Trans. Ind. Applicat, vol. 134, no. 6, pp. 625-663, 2014 (in Japanese).

[22] Q. T. Duong and M. Okada, “Maximum efficiency formulation for inductive power transfer with multiple receivers,” IEICE Electron. Express, vol. 13, no. 22, pp. 20160915, Nov. 2016.

[23] B. H. Waters, P. R. Fidelman, J. D. Raines and J. R. Smith, “Simultaneously Tuning and Powering Multiple Wirelessly Powered Devices,” IEEE WPTC, May. 2015 (DOI: 10.1109/WPT.2015.7140177)

[24] M. Fu *et al*, “Megahertz multiple-receiver wireless power transfer systems with power flow management and maximum efficiency point tracking," IEEE Trans. Microw. Theory Techn., vol. 65, no. 11, pp. 4285–4293, Nov. 2017.

[25] A. Kurs, R. Moffatt and M. Soljačić, “Simultaneous mid-range power transfer to multiple devices," Applied Physics Letters, vol. 96, no. 4, p.044102, 2010

[26] K. K. Eam, B. T. Chuan, T. Imura and Y. Hori, “Impedance matching and power division algorithm considering cross coupling for wireless power transfer via magnetic resonance," IEEE INTELEC 34th International, Oct. 2012 (DOI: 10.1109/INTLEC.2012.6374468)

[27] J. J. Casanova, Z. N. Low and J. Lin, "A loosely coupled planar wireless power system for multiple receivers," IEEE Trans. Ind. Electron., vol. 56, no. 8, pp. 3060–3068, 2009.

[28] S. Lee, S. Kim and C. Seo, "Design of multiple receiver for wireless power transfer using metamaterial," IEEE APMC, Seoul, Korea, Nov. 2013, pp. 1036– 1038.

[29] U. Azad and I. Tzanidis, "Resonant coupling efficiency limits for multiple receivers in a wireless power transfer system," IEEE APSURSI, Orlando, USA, July 2013, pp. 846 – 847.

[30] P. Riehl *et al* "Wireless power systems for mobile devices supporting inductive and resonant operating modes," IEEE Trans. Microw. Theory Tech., vol. 63, no. 3, pp. 780 – 790, 2015.

[31] J. Kim, D. H. Kim and Y. J. Park, "Analysis of capacitive impedance matching networks for simultaneous wireless power transfer to multiple devices," IEEE Trans. Ind. Electron., vol. 62, no. 5, pp. 2807 – 2813, 2015.

[32] X. Liu, C. Wuhan, G. Wang and W. Ding, "Efficient circuit modelling of wireless power transfer to multiple devices," IET Power Electron., vol. 7, no. 12, pp. 3017 – 3022, 2014.

[33] Y. Zhang, Z. Zhao, K. Chen, F. He and L. Yuan, "Wireless power transfer to multiple loads over various distances using relay resonators," IEEE Antennas Wireless Propag. Lett., vol. 25, no. 5, pp. 337 – 339, Mar 2015.

[34] K. Lee, Kunsan, Kunsan and D.-H. Cho, "Analysis of wireless power transfer for adjustable power distribution among multiple receivers," IEEE Antennas Wireless Propag. Lett., vol. 14, pp. 950–953, 2015.

[35] L. J. Chen, J. T. Boys and G. A. Covic, "Power management for multiple-pickup IPT systems in materials handling applications," IEEE Journal of Eerging and Selected Topics in Power Electronics, vol. 3, no. 1, pp. 163–176, 2015.

[36] B. L. Cannon, J. F. Hoburg, D. D. Stancil and S. C. Goldstein, "Magnetic resonant coupling as a potential means for wireless power transfer to multiple small receivers," IEEE Trans. Power Electron., vol. 24, no. 7, pp. 1819–1825, 2009.

[37] J. Kim, H. C. Son, D. H. Kim, and Y. J. Park, “Impedance matching considering cross coupling for wireless power transfer to multiple receivers,” IEEE WPTC, Perugia, Italy, May 2013, pp. 226–229.

[38] A. Sarin, X. Cui and A. T. Avestruz, “Comparison of switched receivers for direct-sequence spread-spectrum wireless power transfer,” IEEE COMPEL, Stanford, CA, USA, July 2017, (DOI: 10.1109/COMPEL.2017.8013359)

[39] D. M. Pozar, Microwave Engineering, 4th ed. John Wiley & Sons, Nov. 2011.

[40] K. Suetake and S. Hayasi, Microwave Circuit, 3th ed. Published by Ohm.co, July. 1961.

Publication List

International Conference

[1] Reona Sugiyama, Duong Quang Thang and Minoru Okada, "Analysis of Maximum Achievable Efficiency in Multiple-Receiver Inductive Power Transfer with Cross-Coupling," 2016 Asian Wireless Power Transfer Workshop (AWPT2016), Dec. 2016
[2] Reona Sugiyama, Duong Quang Thang and Minoru Okada, "kQ-product Analysis of Multiple-Receiver Inductive Power Transfer with Cross-Coupling," 2017 IEEE International Workshop on Antenna Technology IWAT2017, Mar. 2017

Journal(under reviewed)

[3] Reona Sugiyama, Duong Quang Thang and Minoru Okada, "Experimental Evaluation of Maximum Achievable Efficiency for Multiple-Receiver Inductive Power Transfer Systems," IEICE Trans. Fundamentals (Regular EA)